9072 *Biochemistry* **2010,** *49,* 9072–9077
DOI: 10.1021/bi1013547

BIOCHEMISTRY
including biophysical chemistry & molecular biology
Article

A Stereochemical Glimpse of the Active Site of the 8−17 Deoxyribozyme from Iodine-Mediated Cross-Links Formed with the Substrate's Scissile Site†

Gurpreet S. Sekhon and Dipankar Sen*

Department of Molecular Biology and Biochemistry, Simon Fraser University, Burnaby, British Columbia V5A 1S6, Canada

Received April 22, 2010; Revised Manuscript Received September 10, 2010

ABSTRACT: A powerful approach for defining the active site of a complexly folded ribozyme or deoxyribozyme (DNAzyme) is to map the contact cross-links formed between the substrate's reaction site and component residues of the enzyme. Here, we use a novel iodine- and phosphorothioate-mediated method for generating contact cross-links to define key residues of the 8−17 DNAzyme most proximal to the scissile phosphodiester of its bound substrate. Substitution of a phosphorothioate for the scissile phosphodiester renders that site chiral. The cross-linking maps we obtain using chirally resolved substrates give us, for the first time, a stereochemical glimpse of the 8−17's active site. Thus, we identifiy the asymmetric positioning of the DNAzyme's C13 residue, which is catalytically indispensable. We also identify, for the first time, the previously unheralded C3 residue. On the basis of the latter's proximal location to the cleavage site and the impact of its mutation on the DNAzyme's catalytic rate, we hypothesize it may play an acid−base role in the catalysis of the 8−17 DNAzyme. Overall, the approach described in this paper should find wide application in the study of the tertiary folding of RNAs and DNAs, as well as of complexes formed by RNA and DNA with proteins and other ligands.

An interesting approach for identifying nucleobases that participate in forming the active site of a ribozyme or deoxyribozyme (DNAzyme)[1] is the generation of contact cross-links between the site of catalysis within the substrate and its most proximal sites within the ribozyme or DNAzyme. Contact cross-linking is most commonly achieved by photochemical linkage of thio- and halo-substituted nucleobases with other nucleobases (reviewed in ref *1*). For instance, such an approach has been used (*2*, *3*) with success for probing the enzyme−substrate complex of the 8−17 DNAzyme, a small and efficient enzyme for sequence-specific RNA cleavage (reviewed in ref *4*).

Recently, we described a different approach for generating contact cross-links, where the initiating moiety is not a nucleobase but a thio-substituted phosphodiester from the DNA/RNA sugar−phosphate backbone (*5*). Methodologically, this involves the nonphotochemical treatment of a folded DNA/RNA complex, which incorporates a single phosphorothioate, with ethanolic iodine. This is a variant of a procedure which, originally described by Eckstein (*6*), is used for the chemical cleavage of nucleic acids and as a component of sophisticated procedures for studying RNA structure−function (reviewed in ref *7*). We found, however, that several cross-linked species were formed when iodine was used on a phosphorothioate-incorporating enzyme−substrate complex of a photolyase deoxyribozyme, UV1C (*5*, *8*). Mapping of the loci of such iodine-mediated phosophorothioate cross-linking ("IMPC") helped to define the active site as well as aspects of the folding topology of UV1C (the IMPC data obtained were consistent with our earlier photo-cross-linking data on the same system, which had used a well-established methodology (*8*)). The expected chemistry for IMPC, based on the work of Eckstein (*6*), is that the sulfenyl iodide intermediate (containing a P−S−I linkage) is attacked by proximal nucleophiles from DNA nucleobases to generate covalent cross-links. Given that most naturally occurring ribozymes, as well as numerous *in vitro* selected ribozymes and DNAzymes, catalyze condensation/hydrolysis/transesterification reactions of phosphodiesters, such a cross-linking approach should prove especially valuable for identifying ribozyme/DNAzyme residues in the immediate environment of an RNA substrate's reaction site.

One aspect of the chemical structure of DNA/RNA phosphorothioates not explored in our initial study with UV1C is that the phosphorothioate centers are, in fact, chiral. In this study, we wished to use IMPC to more richly define the active site of a small, RNA-cleaving, DNAzyme, the 8−17. Because our initial study did not take advantage of the chirality of phosphorothioates, we wished in particular to obtain a sterically resolved view of the 8−17 active site. The 8−17 DNAzyme is one of the smallest and best characterized of nucleic acid enzymes capable of catalyzing sequence-specific RNA cleavage. A recent review (*4*) reveals that the 8−17 was selected independently at least ten times out of random-sequence DNA libraries using *in vitro* selection (SELEX) (*9*). Some of the variants of the 8−17 reported include the "classic" 8−17 (*9*), which was selected in the presence of magnesium chloride; "Mg5", which was selected in the presence of both magnesium and histidine (*10*); and "17E", which has been shown to be highly active in the presence of zinc (*11*). The 8−17 is able to cleave either a wholly RNA substrate or a DNA substrate with a single ribonucleotide embedded at the cleavage site. Cleavage requires divalent cations at micromolar (Pb^{2+}) to

†This work was supported by Natural Sciences and Engineering Research Council of Canada (NSERC) Grant RGPIN/105785. D.S. is a Fellow of the Canadian Institutes for Advanced Research (CIFAR).

*To whom correspondence should be addressed. E-mail: sen@sfu.ca. Phone: (778) 782-4386. Fax: (778) 782-5583.

[1]Abbreviations: Pu, purine base; Ps, phosphorothioate; Sr, ribose sugar containing substrate; Smet, 2′-*O*-methyl-containing substrate; Sd, deoxyribose-containing substrate; E or DNAzyme, deoxyribonucleotide enzyme; dNTP, deoxynucleoside triphosphate; PAGE, polyacrylamide gel electrophoresis; EDTA, ethylenediaminetetraacetic acid; TBE, Tris−borate−EDTA buffer; TE, Tris−EDTA buffer; NEB, New England Biolabs; IMPC, iodine-mediated phosphorothioate cross-linking; CFQ, charge flow and quenching mapping.

 Published on Web 09/14/2010

millimolar (Mg^{2+}, Ca^{2+}, Mn^{2+}, Zn^{2+}) concentrations. Molar concentrations of certain monovalent cations, such as Li^{+} (but not others, like K^{+}), also support a low level of cleavage (*12*). The folding and catalytic properties of the 8−17 are currently the subjects of extensive study, for which a variety of approaches have been used (reviewed in ref *4*). One of the remarkable findings has been that while substrate cleavage assisted by Mg^{2+} or Zn^{2+} requires a defined global fold of the substrate−DNAzyme complex, a much less extensive local fold of the active site suffices for efficient cleavage with Pb^{2+} (*3*, *13*−*15*).

In the work reported herein, we seek to use IMPC to define further the 8−17 active site. We find that the resolved substrate diastereomers cross-link in a distinguishable fashion to the bound DNAzyme. We are thus able to obtain an unusual, stereochemical view of this DNAzyme's active site.

EXPERIMENTAL PROCEDURES

Oligonucleotides and Enzymes. DNA oligonucleotides were purchased from University of Calgary Core DNA Services and were gel purified prior to use. Phosphodiesterase I from *Crotalus adamanteus* was obtained from Worthington Biochemicals Corp.; nuclease P_1 from *Penicillium citrinum* was from Sigma-Aldrich and from US Biological; calf intestinal alkaline phosphatase was from Roche and polynucleotide kinase from Invitrogen. Terminal transferase was from New England Biolabs. Radionucleotides [γ-^{32}P]ATP and [α-^{32}P]cordycepin were obtained from Perkin-Elmer. All end-labeling reactions were carried out according to the manufacturer's protocols unless otherwise specified.

Reverse-Phase HPLC Purification. Diastereomers of phosphorothioate-incorporated oligonucleotides were separated using reverse-phase HPLC on a Vydac 218TP54 C18 protein and peptide column. The Waters 600 controller contained a U6K manual injector system connected to an Applied Biosystems 759A UV absorbance detector. Solvent A was composed of 5% CH_3CN and 50 mM TEAA, pH 7.4, and solvent B was composed of 30% CH_3CN and 50 mM TEAA, pH 7.4. All buffers were filtered and degassed prior to use. For purification of the Rp and Sp diastereomers of the SrPs substrate (which contains a ribose sugar at the cleavage site) as well as of the SdPs substrate (which contains a deoxyribose sugar at the cleavage site), a linear gradient method was used at 85% A:15% B at time = 0 min to 65% A:35% B at time = 30 min. Purification of the SmetPs substrate (containing a 2′-*O*-methyl sugar at the cleavage site) diastereomers was achieved with a linear gradient of 80% A:20% B at time = 0 min to 65% A:35% B at time = 30 min. Flow rates were 1 mL/min, sparging of all solvents was set to 30 mL/min helium, and temperature was kept constant at 25 °C. The two collected peaks (peak 1 and peak 2) were lyophilized to dryness, redissolved in 25 mL of TE buffer (10 mM Tris, pH 7.4, 0.1 mM EDTA), and subjected to a second round of purification using the same HPLC protocol given above. The oligonucleotide substrates and substrate analogues, SrPs, SmetPs, and SdPs (see Results for more detail) all showed similar chromatograph plots to each other, with minor variations in retention times. Results for the SrPs substrate are shown in Supporting Information Figure S1. The typical substrate diastereomer peak separation was ∼2−3 min dependent on the substrate. The repurification of the separated peaks was necessary as the peaks overlapped somewhat in the initial purification. The two-stage purification resulted in a high level of stereochemical purity (Supporting Information Figure S1) of the Rp and Sp substrates (for instance, 97% purity for *S*- and *R*-SrPs, as determined by HPLC chromatograph analysis. The software Waters Empower 2002 was used to compute peak areas and to estimate levels of cross-contamination).

Characterization of Substrate Diastereomers. The assignment of absolute stereochemistry to the resolved diastereomers of all substrate and substrate analogues was achieved by an established method, which exploits the stereoselective enzymatic activities of venom phosphodiesterase I and nuclease P1 (*15*, *16*). Briefly, Rp phosphorothioate linkages are completely digested to mononucleotides by venom phosphodiesterase but are not digested by nuclease P1 (a dinucleotide linked by a phosphorothioate is left behind). Conversely, Sp phosphorothioates are susceptible to complete digestion by nuclease P1 but not by venom phosphodiesterase I. HPLC-purified substrate diastereomers were treated with 2.5 μg of nuclease P1 in 10 μL of 100 mM Tris, pH 7.2, and 1 mM $MgCl_2$ for 30 min at 37 °C. Separately, purified diastereomers were treated with 25 μg of venom phosphodiesterase I in 10 μL of 100 mM Tris, pH 8.0, and 2 mM $MgCl_2$ for 30 min at 37 °C. Following digestion, all reactions were treated with 20 units of alkaline phosphatase in the dephosphorylation buffer (supplied by Roche, the manufacturer) for an additional 30 min at 37 °C. Nuclease P1 from US Biological was obtained as a powder lyophilized from a solution (30 mM NaOAc, pH 5.3, 5 mM $ZnCl_2$, 50 mM NaCl); for this reason, the manufacturer-recommended digestion protocol was modified. The enzyme was reconstituted in 200 μL of ddH_2O, from which 1 μL was added to the reaction. Twenty microliter reactions in 10 mM NaOAc, pH 5.2 (final concentration), were allowed to react for 1 h at 50 °C. The alkaline phosphatase reaction that followed was buffered to pH 7.8 with 20 mM (final concentration) Tris and allowed to react for 1 h at 37 °C. The mononucleosides and dinucleotides so generated were separated on a C18 column (column and system described above) with the following gradient protocol: 100% solvent C (ddH_2O) at time = 0 min to 80% solvent C and 20% solvent D (70% CH_3CN in ddH_2O) at time = 30 min. The resulting chromatographs for all three substrates proved that peak 1 was the Rp diastereomer and peak 2 was the Sp diastereomer (shown in Supporting Information Figure S2A—E). The mononucleoside retention times were confirmed with alkaline phosphatase-treated dNTP and NTP standards.

Iodine-Dependent Phosphorothioate Cross-Linking. 5′- and 3′-^{32}P-end-labeling of DNA was carried out using polynucleotide kinase and terminal transferase, respectively, using protocols provided by the respective manufacturers.

Cross-linking reactions were carried out in total reaction volumes of 12 μL. First, 1 mM (final reaction concentrations) each of E and phosphorothioate-containing substrate analogue (including trace amounts of either 5′- or 3′-^{32}P-labeled E) was heated, in 6 μL of TE buffer, to 94 °C for 30 s and allowed to cool to room temperature (21 °C). After 10 min, 2 μL of appropriate buffer stocks was added to give final salt and DNA concentrations. After 1 min, 2 μL of I_2 in EtOH was added to a final concentration of 30 μM. The iodine reaction proceeded for 1 min and was stopped with an equal volume of formamide-containing loading solution for denaturing gels. Following heat denaturation at 100 °C, the DNA solutions were loaded onto denaturing 12% polyacrylamide gels.

Hydroxyl Radical Footprinting. Hydroxyl radical-mediated footprinting was carried using the method of Tullius (*17*) by way

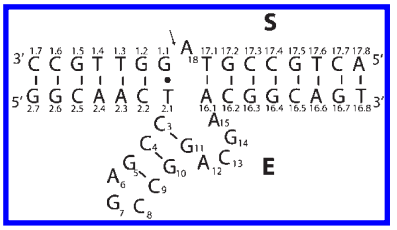

FIGURE 1: The sequence of S, the substrate (and substrate analogues), and the sequence and secondary structure of E, the 8−17 deoxyribozyme used in this study. The arrow indicates the cleavage site. All substrates contain a phosphorothioate modification that replaces a nonbridging oxygen with sulfur at the scissile site (A18). The two substrate analogues, SdPs and SmetPs, contain 2′-deoxyribose and 2′-methoxydeoxyribose, respectively, at A18. The rest of these substrates are DNA. The SrPs substrate has a ribose sugar at A18. Watson−Crick base pairs are shown with solid lines, and the single wobble pair is shown with a dot.

of Fenton reaction-generated hydroxyl radicals. Gel-purified samples of cross-linked or control DNAs were eluted into TE buffer, ethanol precipitated, and redissolved in 10 μL of TE. Prior to initiating reactions, fresh reagent stocks of 1 mM $(NH_4)_2Fe(SO_4)_2 \cdot 6H_2O$ + 2 mM EDTA, pH 8.0, 10 mM ascorbate, 3% H_2O_2, and 100 mM thiourea were prepared and kept on ice. One microliter drops of each prepared reagent (except thiourea) were placed on the inside edge of sample tubes. To initiate the Fenton reaction, all three drops were quickly mixed on the tube wall and pipet-mixed into the DNA solution. After 5 min, reactions were stopped with 1 μL of the thiourea reagent. Following lyophilization, the Fenton-cleaved products were dissolved in denaturing loading buffer, denatured at 100 °C, and run in 15% denaturing polyacrylamide gels.

Guanine-, cytosine-, and thymine-specific chemical sequencing ladders were generated using standard chemical modification techniques (*18*).

Gel Analysis. Phosphorimagery was carried out using Fuji phosphor screens, which were scanned in a Molecular Dynamics Typhoon 9410 variable mode imager. Quantitative analysis was carried out using the NIH ImageJ software.

RESULTS AND DISCUSSION

Figure 1 shows the nucleotide sequences of the substrate (and substrate analogues) and the version of the 8−17 deoxyribozyme used in this study. The arrow indicates the scissile site. The term "E" refers to the unmodified 8−17 DNAzyme, as shown in Figure 1. Substrate ("S") analogues incorporating single phosphorothioate residues at the scissile site are referred to respectively as SdPs and SmetPs (in SdPs, the sugar of the A18 nucleotide is a deoxyribose; in SMetPs, it is 2′-methoxyribose). Resolved diastereomers of SdPs (or SmetPs) are referred to as Rp and Sp, respectively, in reference to the chirality of their phosphorothioate moieties, while M refers to the unresolved, racemic, mixture of the two.

Figure 2A shows that iodine treatment of the E DNAzyme complexed with either SdPs or SmetPs generates cross-linked products (slow-moving species, relative to the un-cross-linked enzyme). We showed them to be *inter*molecularly cross-linked species, containing both DNAzyme and substrate, by cross-labeling experiments, in which radiolabeled DNAzyme complexed with unlabeled substrate, and vice versa, gives rise to the same cross-linked product bands (Supporting Information Figure S3).

Figure 2A highlights the different cross-linked products generated from 5′- and, separately, 3′-radiolabeled E complexed, in the

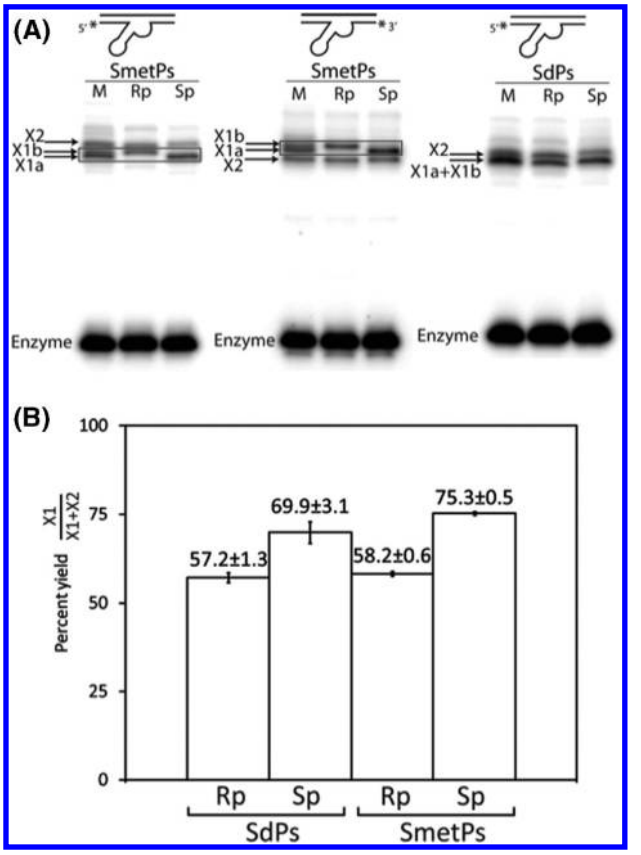

FIGURE 2: The products from iodine-mediated phosphorothioate cross-linking (IMPC) experiments using, separately, the substrate analogues SmetPs and SdPs. (A) In each case, the substrate is racemic (M) or a purified diastereomer (Rp or Sp). X1a, X1b, and X2 show cross-linked DNAzyme−substrate products. (B) The yield of X1 (the sum of X1a and X1b) plotted as a percentage of the total yield of cross-linked products (X1 + X2). The data shown refer to the sets of experiments in which the DNAzyme is 5′-labeled. Error bars report the range between the two independent sets of data.

presence of 10 μM Na^+ and 10 μM Mg^{2+}, with (a) the racemic mixture ("M") of substrates SdPs and SmetPs and (b) to the Rp and the Sp versions of these two substrates (none of the substrates is radiolabeled in these experiments). Inspection of the SmetPs/M lane (where the enzyme is labeled on its 5′-end, extreme left) shows three major cross-linking products, designated X1a, X1b, and X2, respectively. Comparison of products from the corresponding lanes that feature the 5′- and the 3′-labeled enzyme permits the assignment of individual cross-linked products in the two lanes. Thus, while the X1a and X1b products move faster than X2 with a 5′ end-label on the enzyme, they move slower than X2 with a 3′ end-label on the enzyme. An interesting observation is that within a set of three lanes (such as from 5′-labeled enzyme cross-linked to racemic and resolved SmetPs) the X1b product of SmetPs-M migrates comparably to the faster product of SmetPs-Rp, and the X1a product of SmetPs-M migrates comparably to the faster product of SmetPs-Sp. A reasonable hypothesis then is that the X1a and X1b cross-linked products share a linkage and are only stereochemically distinct from each other. Analogous support for this hypothesis is offered also by the cross-linked products generated from the 3′-end-labeled SmetPs. By contrast, the X2 species from the Rp substrate runs comparably to the X2 species from the Sp substrate (as well as from the racemic substrate mixture, M).

With regard to cross-linked products formed from the 5′-end-labeled SdPs substrate, the X1a and X1b products are not so well

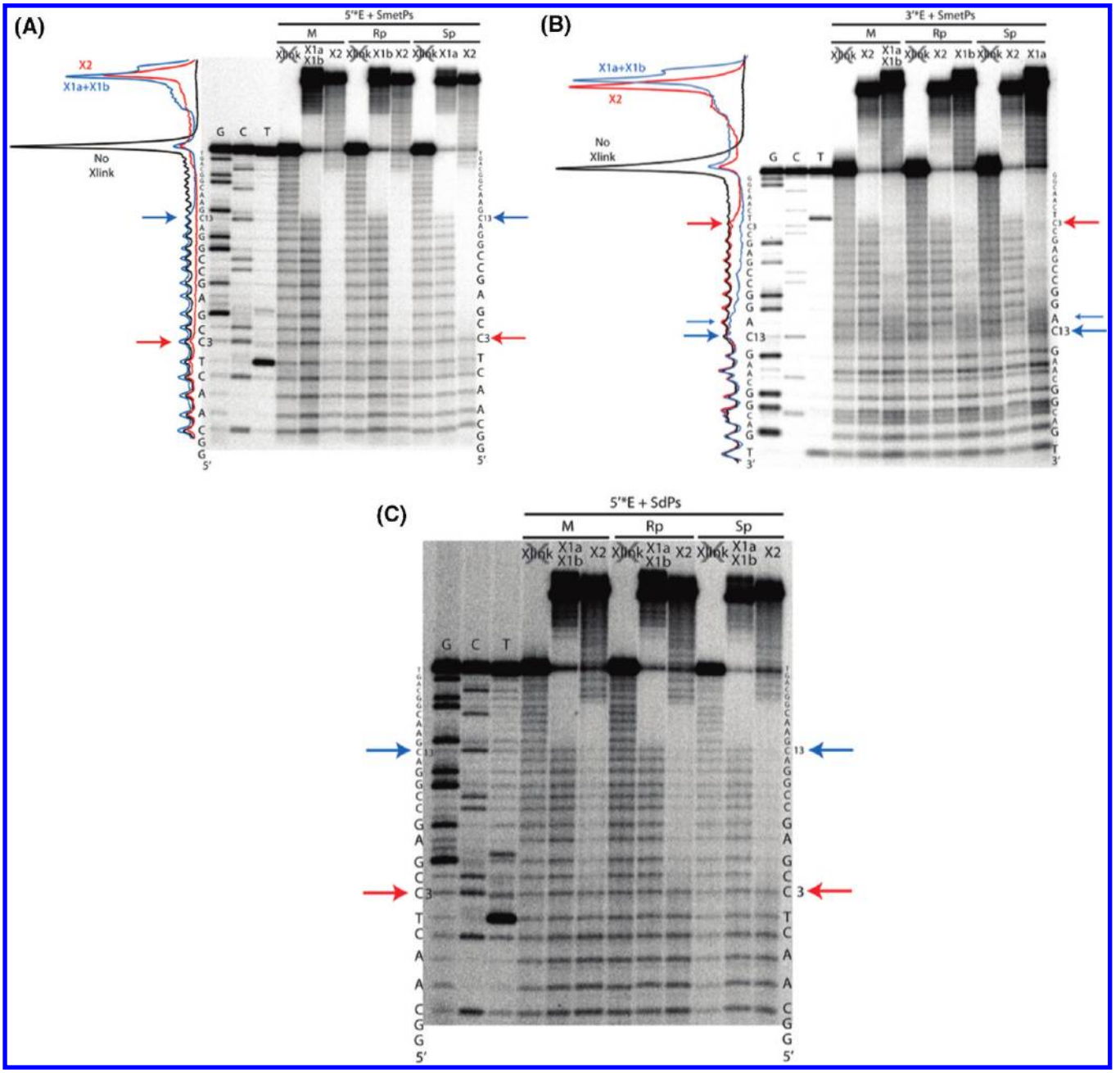

FIGURE 3: Hydroxyl radical footprinting of E, complexed with SmetPs or with SdPs, and then subjected to either cross-linking or not. (A) Unlabeled SmetPs complexed with 5′-^{32}P-labeled E. (B) Unlabeled SmetPs complexed with 3′-^{32}P-labeled E. (C) Unlabeled SdPs complexed with 5′-^{32}P-labeled E. Densitometry plots are shown on the left, referring only to the data in the M lanes. The arrows identify discontinuities in the hydroxide radical generated ladders, indicating sites of cross-linking.

separated from each other, although they continue to run distinctly from the X2 product. Figure 2B tabulates data from two independent cross-linking experiments. Although the absolute yields of cross-linked products is small in any given experiment, the ratios of the different cross-linked products are found to be highly reproducible. The ratios of the different cross-linked products formed from both E-SdPs and E-SmetPs complexes (each comprised of 5′-^{32}P-labeled E complexed with the unlabeled substrate) highlight two observations: (a) The cross-link yields for X1a plus X1b (plotted in Figure 2b as "X1") are reproducibly higher than for X2 [i.e., X1/(X1 + X2) > 50%], regardless of the identity or the stereochemistry of the substrate. This is highly suggestive of the DNAzyme nucleophile responsible for X1a/b occupying a more proximal location for attack on the substrate's sulfenyl iodide than the nucleophile responsible for X2. (b) The notably, and reproducibly, higher X1/(X1 + X2) values seen with the Sp substrate, relative to the Rp substrate, are consistent with the nucleophile responsible for X1a/b occupying a more *asymmetric* location (compared to the location of the X2 nucleophile) in relation to the substrate phosphorothioate.

To map the precise sites of cross-linking within the DNAzyme, hydroxyl radical-mediated footprinting of the cross-linked complexes was carried out. This is a variant of a standard methodology used to identify the location of a cross-link within a given end-labeled DNA or RNA, and it does not require either the chemical identification or reversal of the cross-link itself. In a typical case, we generate a cross-linked species using 5′-radiolabeled E bound to nonradiolabeled S. Fenton reaction-generated hydroxyl radicals in situ can then be used to generate strand breaks in the ensemble of cross-linked molecules, such that any

individual cross-linked molecule receives either zero or one strand break within it (*20*). Analysis by denaturing gel electrophoresis then shows a continuous nucleotide ladder that stretches from the 5′-end of E to the site of cross-linking (at which point there is an abrupt interruption in the ladder, owing to the much higher molecular weight of the next smallest cleaved species, which now includes the cross-linking site itself as well as one or more unbroken arm of E and S). Likewise, 3′ radiolabeling of E, within the same E−S cross-linked species, generates a ladder stretching from the 3′-end of E to the precise point of cross-linking. It is possible to use the Fenton reaction to identify unambiguously the site of cross-linking (in relation to a Maxam−Gilbert sequence ladder). In both the Fenton and Maxam−Gilbert lanes, a band representing a nucleotide at position X (say, relative to the 5′-end) will contain DNA inclusive of the nucleotide X + 1, as well as the phosphate residue that had linked X to X + 1 (*17*, *18*).

Panels A and B of Figure 3 show respectively footprinting results from the cross-linked products of 5′- and 3′-end-labeled E (complexed, in turn, to the M, Sp, and Rp versions of SmetPs). In confirmation of the above hypothesis that X1a and X1b are stereroisomers, they both map to the same DNAzyme nucleobase, C13 in the bulge loop (see Figure 1). It was not possible to separate the X1a and X1b products of the M substrate from each other; they are therefore footprinted within a single lane. However, comparison of densitometric plots (shown to the left of the gels in Figure 3A,B) from footprinting of [X1a + X1b]-M (shown in blue) relative to [un-cross-linked DNAzyme]-M (shown in black) reveals (a) that the precise site of cross-linking is C13 (although, from Figure 3B, there is some indication that A12, too, may be a participant) and (b) that there are no additional intensity maxima and minima in the X1a and X1b footprints; in other words, there is unlikely to be a second cross-linking site buried in the data. Similarly, the X2 product clearly identifies C3 of the DNAzyme as its cross-linking site (confirmed by the red densitometric plot in Figure 3A,B). Figure 3C shows that cross-link site mapping of E linked to the SdPs substrate maps identical cross-linking sites as those seen with the SmetPs substrate.

To summarize the above cross-linking data: we have found that the C13 base makes the X1a,b cross-links, whereas the C3 base on the DNAzyme makes the X2 cross-link. The formation of cross-links between the DNAzyme's C3 and C13 residues with the substrate's scissile phosphorothioate as well as the differential cross-linking of the C13 residue with the Rp and the Sp diastereomers of the substrate (a) offers a stereochemical glimpse of the 8−17 active site and (b) identifies a previously unheralded cytosine, C3, as a likely player in the 8−17 catalytic mechanism. Figure 4 conceptualizes the relative positioning of the C13 and C3 residues in relation to the substrate's scissile site. Our data show that C13 cross-links more heavily with the Sp sulfur and is likely to be located closer to it than to the Rp sulfur. From the present data it is not possible to locate the C3 residue with confidence in relation to the phosphorothioate residue. However, the C3 residue is clearly proximal to the phosphorothioate, given the ready formation of the X2 cross-link.

A rate−pH profile measurement for the 8−17 DNAzyme has shown that it has a functionally linked pK_a around neutral pH (*21*); this is consistent with (although it does not prove) the existence of a nucleobase with acid−base properties relevant to the cleavage mechanism. A similar property has also been reported for the HDV ribozyme, whose C75 nucleobase has been shown to act as a cleavage-relevant general acid (*22*−*25*).

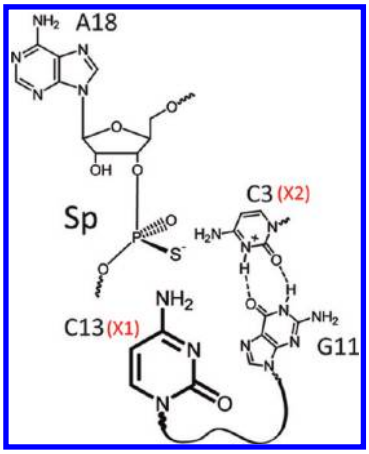

FIGURE 4: A model illustrating the postulated position of the C13 DNAzyme base in relation to the scissile phosphorothioate. The Sp diastereomer of the substrate is shown. The G11-C3 base pair is portrayed as a wobble to show a putatively protonated C3. The C3 base is shown to be proximal to the phosphorothioate; however, its exact location remains undefined.

The identification of C3 as a major cross-linking partner for the scissile site offers the possibility that this nucleobase acts as a general acid−base in the 8−17 catalytic reaction. Earlier mutagenesis studies had found that mutating the C3-G11 base pair to a G3-C11 base pair decreases cleavage activity 2−5-fold, while mutating it to A3-T11 or to T3-A11 reduces activity by 1 and 2 orders of magnitude, respectively (*19*). It is plausible then to hypothesize that Watson−Crick stabilization of the 3 bp minihelix within the 8−17 catalytic core might not be the only role for the C3-G11 pair and that C3 may be protonated/deprotonated in the course of the 8−17's catalytic cycle. The mutational data, above, are consonant with such an acid−base role of C3; the C-G to A-T mutation lowers cleavage activity by an order of magnitude, consistent with the intrinsic pK_a difference between cytosine and adenine (*22*−*25*). Mutation of the C-G to a G-C pair could preserve the acid−base role of the cytosine, except make it less effective by virtue of being shifted away from its optimal positioning.

Our earlier study using photo-cross-linking had shown that the C13 base did cross-link in the region of the scissile site in the substrate (*2*). C13 is an invariant residue (*19*), critically required for the catalytic activity of the 8−17 DNAzyme. A quite different study also found a distinctive chemical and electronic behavior of C13. Leung and Sen (*26*) studied the pattern of charge (electron hole) migration through the folded 8−17 DNAzyme−substrate complex and identified C13 as having both a high solvent accessibility and a nontypical electronic environment relative to other cytosines within the DNAzyme−substrate complex. Thus, for instance, its radical cation reacted at a high level with water to give undefined oxidized cytosine species, which were susceptible to hydrolysis upon treatment with aqueous base (*intra*helical cytosines in DNA typically do not show this property) (*26*). The IMPC data presented here corroborate those earlier findings that C13 is located in a unique structural/electronic arrangement within the folded DNAzyme−substrate complex. Further studies will undoubtedly shed light on the detailed roles played by the C3 and C13 nucleobases within this interesting catalytic system.

In conclusion, we anticipate that the IMPC methodology, as described in this paper, should be broadly applicable to the study of the tertiary folding of DNAs as well as RNAs and also find valuable use in the study of complexes formed by RNAs and DNAs with proteins and other ligands.

ACKNOWLEDGMENT

We are grateful to Yong Liu and the members of the Sen Laboratory for valuable discussions.

SUPPORTING INFORMATION AVAILABLE

Identification of stereospecific substrates by enzymatic digestion and RP-HPLC (Figures S1 and S2A−E) and cross-labeling experiment with either DNAzyme 5′-end-labeled or substrate 5′-end-labeled (Figure S3). This material is available free of charge via the Internet at http://pubs.acs.org.

REFERENCES

1. Favre, A., Saintomé, C., Fourrey, J. L., Clivio, P., and Laugâa, P. (1998) Thionucleobases as intrinsic photoaffinity probes of nucleic acid structure and nucleic acid-protein interactions. *J. Photochem. Photobiol. B 42*, 109–124.
2. Liu, Y., and Sen, D. (2008) A contact photo-cross-linking investigation of the active site of the 8−17 deoxyribozyme. *J. Mol. Biol. 381*, 845–859.
3. Liu, Y., and Sen, D. (2010) Local rather than global folding enables the lead-dependent activity of the 8−17 deoxyribozyme: Evidence from contact photo-cross-linking. *J. Mol. Biol. 395*, 234–241.
4. Schlosser, K., and Li, Y. (2010) A versatile endoribonuclease made of DNA: Characteristics and applications of the 8−17 DNAzyme. *ChemBioChem 16*, 311–322.
5. Sekhon, G. S., and Sen, D. (2009) Unusual DNA-DNA cross-links between a photolyase deoxyribozyme, UV1C, and its bound oligonucleotide substrate. *Biochemistry 48*, 6335–6347.
6. Gish, G., and Eckstein, F. (1988) DNA and RNA sequence determination based on phosphorothioate chemistry. *Science 240*, 1520–1522.
7. Cochran, J. C., and Strobel, S. A. (2004) Probing RNA structure and function by nucleotide analog interference mapping. *Curr. Protoc. Nucleic Acid Chem.*, Chapter 6, Unit 6.9.
8. Chinnapen, D. J., and Sen, D. (2004) A deoxyribozyme that harnesses light to repair thymine dimers in DNA. *Proc. Natl. Acad. Sci. U.S.A. 101*, 65–69.
9. Santoro, S. W., and Joyce, G. F. (1997) A general purpose RNA-cleaving DNA enzyme. *Proc. Natl. Acad. Sci. U S A 94*, 4262–6.
10. Faulhammer, D., and Famulok, M. (1997) Characterization and divalent metal-ion dependence of *in vitro* selected deoxyribozymes which cleave DNA/RNA chimeric oligonucleotides. *J. Mol. Biol. 269*, 188–202.
11. Li, J., Zheng, W., Kwon, A. H., and Lu, Y. (2000) In vitro selection and characterization of a highly efficient Zn(II)-dependent RNA-cleaving deoxyribozyme. *Nucleic Acids Res. 28*, 481–488.
12. Mazumdar, D., Nagraj, N., Kim, H.-K., Meng, X., Brown, A. K., Su, Q., Li, W., and Lu, Y. (2009) Activity, folding and Z-DNA formation of the 8−17 DNAzyme in the presence of monovalent ions. *J. Am. Chem. Soc. 131*, 5506–5515.
13. Brown, A. K., Jing, L., Pavot, C. M.-B., and Lu, Y. (2003) A lead-dependent DNAzyme with a two-step mechanism. *Biochemistry 42*, 7152–7161.
14. Kim, H.-K., Liu, J., Li, J., Nagraj, N., Li, M., Pavot, C. M.-B., and Lu, Y. (2007) Metal-dependent global folding and activity of the 8−17 DNAzyme studied by fluorescence resonance energy transfer. *J. Am. Chem. Soc. 129*, 6896–6902.
15. Bryant, F. R., and Benkovic, S. J. (1979) Stereochemical course of the reaction catalyzed by 5′-nucleotide phosphodiesterase from snake venom. *Biochemistry 18*, 2825–2828.
16. Potter, B. V. L., Connolly, B. A., and Eckstein, F. (1983) Synthesis and configurational analysis of a dinucleoside phosphate isotopically chiral at phosphorus. Stereochemical course of *Penicillium citrinum* nuclease P1 reaction. *Biochemistry 22*, 1369–1377.
17. Tullius, T. D., and Greenbaum, J. A. (2005) Mapping nucleic acid structure by hydroxyl radical cleavage. *Curr. Opin. Chem. Biol. 9*, 127–134.
18. Maxam, A. M., and Gilbert, W. (1977) A new method for sequencing DNA. *Proc. Natl. Acad. Sci. U.S.A. 74*, 560–564.
19. Peracchi, A., Bonaccio, M., and Clerici, M. (2005) A mutational analysis of the 8−17 deoxyribozyme core. *J. Mol. Biol. 352*, 783–794.
20. Sontheimer, E. J. (1994) Site-specific RNA crosslinking with 4-thiouridine. *Mol. Biol. Rep. 20*, 35–44.
21. Bonaccio, M., Credali, A., and Peracchi, A. (2004) Kinetic and thermodynamic characterization of the RNA-cleaving 8−17 deoxyribozyme. *Nucleic Acids Res. 32*, 916–925.
22. Ferre-D'Amare, A., Zhou, K., and Doudna, J. A. (1998) Crystal structure of a hepatitis delta virus ribozyme. *Nature 395*, 567–574.
23. Nakano, S., Chadalavada, D. M., and Bevilacqua, P. C. (2000) General acid-base catalysis in the mechanism of the hepatitis delta virus ribozyme. *Science 287*, 1493–1497.
24. Shih, I. H., and Been, M. D. (2002) Catalytic strategies of the hepatitis delta virus ribozymes. *Annu. Rev. Biochem. 71*, 887–917.
25. Cerrone-Szakal, A. L., Siegfried, N. A., and Bevilacqua, P. C. (2008) Mechanistic characterization of the HDV genomic ribozyme: Solvent isotope effects and proton inventories in the absence of divalent metal ions support C75 as the general acid. *J. Am. Chem. Soc. 130*, 14504–14520.
26. Leung, E. K. Y., and Sen, D. (2007) Electron hole flow patterns through the RNA cleaving 8−17 deoxyribozyme yield unusual information about its structure and folding. *Chem. Biol. 14*, 41–51.